NAVAL POSTGRADUATE SCHOOL

MONTEREY, CALIFORNIA

THESIS

ASSESSING THE OPERATIONAL RESILIENCE OF ELECTRICAL DISTRIBUTION SYSTEMS

by

Clark Petri

September 2017

Thesis Co-Advisors:	David Alderson
	W. Matthew Carlyle
Second Reader:	Jeffrey Appleget

Approved for public release. Distribution is unlimited.

THIS PAGE INTENTIONALLY LEFT BLANK

REPORT DOCUMENTATION PAGE

Form Approved OMB No. 0704–0188

Public reporting burden for this collection of information is estimated to average 1 hour per response, including the time for reviewing instruction, searching existing data sources, gathering and maintaining the data needed, and completing and reviewing the collection of information. Send comments regarding this burden estimate or any other aspect of this collection of information, including suggestions for reducing this burden to Washington headquarters Services, Directorate for Information Operations and Reports, 1215 Jefferson Davis Highway, Suite 1204, Arlington, VA 22202–4302, and to the Office of Management and Budget, Paperwork Reduction Project (0704-0188) Washington DC 20503.

1. AGENCY USE ONLY *(Leave Blank)*	2. REPORT DATE	3. REPORT TYPE AND DATES COVERED
	September 2017	Master's Thesis 06-25-2015 to 09-22-2017

4. TITLE AND SUBTITLE

ASSESSING THE OPERATIONAL RESILIENCE OF ELECTRICAL DISTRIBUTION SYSTEMS

5. FUNDING NUMBERS

6. AUTHOR(S)

Clark Petri

7. PERFORMING ORGANIZATION NAME(S) AND ADDRESS(ES)

Naval Postgraduate School
Monterey, CA 93943

8. PERFORMING ORGANIZATION REPORT NUMBER

9. SPONSORING / MONITORING AGENCY NAME(S) AND ADDRESS(ES)

N/A

10. SPONSORING / MONITORING AGENCY REPORT NUMBER

11. SUPPLEMENTARY NOTES

The views expressed in this document are those of the author and do not reflect the official policy or position of the Department of Defense or the U.S. Government. IRB Protocol Number: N/A.

12a. DISTRIBUTION / AVAILABILITY STATEMENT

Approved for public release. Distribution is unlimited.

12b. DISTRIBUTION CODE

13. ABSTRACT *(maximum 200 words)*

Electrical distribution systems are the last stage of electricity delivery, bridging the gap between transmission networks and the customer. Compared to transmission systems, there has been comparatively little analysis performed on distribution infrastructure. We first establish a minimum load shed optimal switching model. The model seeks to ensure all electricity demand is met for a given distribution system by minimizing the amount of load not met. This is accomplished by closing and opening switches within the network, subject to various electrical physics constraints. We initially test our model against a simple toy network to verify proper operation before expanding to increasingly complex networks. We culminate with testing against a standardized test circuit.

The model runs in an open-source programming language on a consumer-grade laptop, reading in data from common formats with solvers readily familiar to the optimization community.

14. SUBJECT TERMS

electrical distribution, disruption, optimal switching model, outage, three phase, linearized flow, optimization, Python, Pyomo, infrastructure

15. NUMBER OF PAGES 55

16. PRICE CODE

17. SECURITY CLASSIFICATION OF REPORT	18. SECURITY CLASSIFICATION OF THIS PAGE	19. SECURITY CLASSIFICATION OF ABSTRACT	20. LIMITATION OF ABSTRACT
Unclassified	Unclassified	Unclassified	UU

NSN 7540-01-280-5500

Standard Form 298 (Rev. 2–89)
Prescribed by ANSI Std. 239–18

THIS PAGE INTENTIONALLY LEFT BLANK

Approved for public release. Distribution is unlimited.

ASSESSING THE OPERATIONAL RESILIENCE OF ELECTRICAL DISTRIBUTION SYSTEMS

Clark Petri
Lieutenant Commander, United States Navy
B.S., Oregon State University, 2005

Submitted in partial fulfillment of the
requirements for the degree of

MASTER OF SCIENCE IN OPERATIONS RESEARCH

from the

NAVAL POSTGRADUATE SCHOOL
September 2017

Approved by: David Alderson
Thesis Co-Advisor

W. Matthew Carlyle
Thesis Co-Advisor

Jeffrey Appleget
Second Reader

Patricia Jacobs
Chair, Department of Operations Research

THIS PAGE INTENTIONALLY LEFT BLANK

ABSTRACT

Electrical distribution systems are the last stage of electricity delivery, bridging the gap between transmission networks and the customer. Compared to transmission systems, there has been comparatively little analysis performed on distribution infrastructure. We first establish a minimum load shed optimal switching model. The model seeks to ensure all electricity demand is met for a given distribution system by minimizing the amount of load not met. This is accomplished by closing and opening switches within the network, subject to various electrical physics constraints. We initially test our model against a simple toy network to verify proper operation before expanding to increasingly complex networks. We culminate with testing against a standardized test circuit.

The model runs in an open-source programming language on a consumer-grade lap-top, reading in data from common formats with solvers readily familiar to the optimization community.

THIS PAGE INTENTIONALLY LEFT BLANK

Table of Contents

1 Introduction **1**
1.1 The Importance of Electric Power 1
1.2 Thesis Structure 3

2 Background **5**
2.1 Technical Background Overview 5
2.2 Previous Research 6

3 Model **11**
3.1 Model Formulation 11
3.2 Model Implementation 16
3.3 Model Testing 17
3.4 Model Performance on Basic Test Circuit 17
3.5 Model Testing With Cycles 18
3.6 Model Performance on Basic Test Circuit with Cycle 20
3.7 Model Validation 21

4 Results **23**
4.1 IEEE RTS 13-bus feeder 23
4.2 IEEE 13 Node Test Feeder Performance 25
4.3 Expansion of IEEE 13 Node Test Feeder 27
4.4 Model Performance Overview 28

5 Conclusions and Follow-on Work **29**
5.1 Conclusions 29
5.2 Follow-on Work 29

List of References **31**

Initial Distribution List **35**

List of Figures

Figure 3.1 Basic Test Circuit 17

Figure 3.2 Basic Test Circuit with Cycle 19

Figure 4.1 IEEE 13 Node Test Feeder 23

Figure 4.2 Duplicated 13 Node Test Feeder 27

THIS PAGE INTENTIONALLY LEFT BLANK

List of Tables

Table 3.1 Basic Test Circuit Node Data 18

Table 3.2 Basic Test Circuit Edge Data 18

Table 3.3 Basic Test Circuit with Cycle Node Data 19

Table 3.4 Basic Test Circuit with Cycle Edge Data 20

Table 3.5 Basic Test Circuit with Cycle Results before Cycle Breaking Constraint 20

Table 3.6 Basic Test Circuit with Cycle Results after Cycle Breaking Constraint 21

Table 4.1 IEEE 13 Node Test Feeder Node Data 24

Table 4.2 IEEE 13 Node Test Feeder Edge Data 25

Table 4.3 IEEE 13 Node Test Feeder Edge Results 26

Table 4.4 Duplicated IEEE 13 Node Test Feeder Edge Results 28

THIS PAGE INTENTIONALLY LEFT BLANK

List of Acronyms and Abbreviations

AC Alternating Current

ACPF Alternating Current Power Flow

AD Attacker-Defender

DAD Defender-Attacker-Defender

DHS Department of Homeland Security

DOD Department of Defense

EE Electrical Engineering

EMP Electromagnetic Pulse

GPA Guam Power Authority

GUI Graphical User Interface

IEEE Institute of Electrical and Electronics Engineers

JSON JavaScript Object Notation

JWAC Joint Warfare Analysis Center

Kv Kilovolts

Kvar Kilovolt-ampere reactive

Kw Kilowatts

LANL Los Alamos National Laboratory

LP Linear Programming

MIP Mixed-integer program

Mw Megawatts

NPS Naval Postgraduate School

OR Operations Research

PG Power Grid

RTS Reliability Test System

USN U.S. Navy

VEGA Vulnerability of Electric Grids Analyzer

Executive Summary

Of the 16 critical infrastructure sectors, electric power is identified as being significantly important because it enables the operation of the other sectors. Within the realm of electric power, electrical distribution systems consist of the substations, transformers, and lines that bridge the gap between transmission systems, which originate at power plants such as coal or nuclear, and the end-user. Distribution systems are most readily characterized as the power poles and lines running between homes, commercial businesses, and neighboring municipalities.

Working in concert with our associates at Los Alamos National Labs (LANL) and under the Joint Warfare Analysis Center (JWAC) - NPS research program, we build a linearized optimization model in the Python programming language, implementing the mathematical program in the Pyomo environment. The original formulation was provided by our LANL associates and expanded upon during model development. At its core, the model delivers real and reactive power from an originating substation(s) to loads throughout the network, adhering to various electrical engineering physics constraints.

These constraints include flow balance, balance between the power transmission for phases within a single line, adhering to the thermal limits of lines, line losses due to resistance and reactance, maintaining nominal system operating voltage, and various topology constraints. The entire model is driven by an objective function seeking to minimize the load shed throughout the network.

Testing and analysis is initially performed on a test circuit provided by our associates at LANL. The circuit is simple enough that basic operation can be checked by hand calculation to verify model behavior. We then specifically examine behavior of the topology constraints against another test circuit we designed. We observe the model performing proper operation of switches within the network to preclude cycle formation while still minimizing load shed.

Our testing culminates with application of an Institute of Electrical and Electronics Engineers (IEEE) standardized test circuit. The test circuit possesses more robust and dynamic electrical characteristics, specifically imbalanced loading and phase variations. Zero load shed is expected with the test circuit and we observe none with our model. The downstream

goal of our work here is to perform analysis on real-world distribution systems when they are subject to various disruptions. As an intermediate step toward that goal we duplicate the IEEE network into “a” and “b” sides, connecting them with a single line containing a switch. We proceed to remove the substation from the “b” side and observe the resulting behavior as the remaining “a” substation attempts to power the entire system.

We conclude with recommendations for continued work and analysis. Specifically, our model can be folded into attacker-defender analyses to inform researchers on vulnerabilities within a given distribution system. Furthermore, testing of real-world systems by triggering systematic failures of given components can yield insights to distribution system behavior when under duress. Our work is unique due to its focus on distribution systems, its adherence to electrical engineering mathematics, and results with guaranteed optimality.

Acknowledgments

I am forever thankful to Dr. David Alderson. Thank you for your guidance during not only my thesis work but the entirety of the curriculum here. Your enthusiasm for the material, insight and mentorship kept me going and also provided inspiration to keep striving, despite frequently feeling out of my element. "Stay to the left" became a mantra for me and often the source of many a wry smile between us. As I continue in my career I will consistently seek to emulate your attention to detail and ability to quickly frame and solve a problem. Thank you, Sir.

A special debt of gratitude is owed to Dr. Matthew Carlyle, who exhibited saint-like patience in his tireless efforts to help me grasp the material. The quality of your teaching is impeccable and is the reason why I consistently sought out your classes, despite my frequent intimidation. Many thanks are in order for making networks, mathematical programming, and optimization proofs cool, and you know what type of cool I mean.

Special thanks go to Dr. Jeffrey Appleget. I never could have imagined that an innocent inquiry regarding megacities would lead me to the JWAC - NPS Research partnership and subsequently down this path, but I am thankful I talked to you a year ago.

A big thank you to Harsha Nagarajan, Arthur Barnes, and Scott Backhaus from Los Alamos National Labs. Despite your various projects, you always found time to help me with this thesis. Thank you for your hospitality when I visited and your continued insight these many months.

I would remiss to not mention a few key members of my cohort, namely Adam Hepworth, Ezra Akin, Scott Cohick, Charles Clark, Lee Huffstetler, and Matt Schaefer. Whether you knew it or not, each of you in your own ways offered me encouragement, help, and inspiration to always push harder.

Lastly, there is my amazing wife, Sherri. You watched me stumble and fall countless times these last two years but were always there to help me up and keep going. Your support, encouragement, and love made this possible and I am forever thankful for your strength. You are my best friend and biggest supporter – I love you.

THIS PAGE INTENTIONALLY LEFT BLANK

CHAPTER 1:
Introduction

The U.S. government defines critical infrastructure as "systems and assets, whether physical or virtual, so vital to the United States that the incapacity or destruction of such systems and assets would have a debilitating impact on security, national economic security, national public health or safety, or any combination of those matters" (White House, 2013). Critical infrastructure systems are those which deliver the energy to heat and cool our homes, the water we drink, the communication systems we enjoy, and the transportation systems that are integral to the American way of life. Furthermore, these systems serve as the foundation for the economy, security, and health of our nation (Department of Homeland Security, 2017). Due to the significance of these systems, there is considerable interest in understanding, modeling, and predicting of infrastructure system response to disruption. It is of paramount interest at the presidential level that we "maintain secure, functioning, and resilient critical infrastructure" (White House, 2013). Electric power, one of these critical infrastructure systems, is the focus of this research.

1.1 The Importance of Electric Power

As defined by the Department of Homeland Security (DHS), there are 16 critical infrastructure sectors (Department of Homeland Security, 2017). Of these, electric power is particularly important because it provides an "enabling function" for the others in fundamental ways (White House, 2013).

The overall structure of electrical power infrastructure can be loosely categorized into three main parts: generation, transmission, and distribution. Generation systems, such as solar, hydro, wind, nuclear, or gas turbine power plants, produce electricity. Transmission systems move electricity in bulk from the originating power plant to substations and are most commonly recognized as the massive towers carrying heavy lines across rural stretches of highway. The distribution system exists between the substation and end customer, most readily characterized as the telephone poles abundant in any residential and commercial area.

Disruptions to the electric power system can be caused by a variety of sources. Foremost among these are natural disasters such as hurricanes or earthquakes. For example, Hurricane Sandy in 2012 caused power losses to over 8,000,000 homes across 17 states (Webley, 2012). Other potential causes of electric power disruption are operator error (e.g., the Three Mile Island incident; see Nuclear Regulatory Commission, 2013) or the actions of an adversary (e.g., the coordinated attacks on the Metcalf substation in 2013 near San Jose, CA; see Smith, 2014). Consequences for these disruptions vary depending on the scope and scale of the damage as well as the types of electricity infrastructure damaged. A car hitting a power pole may interrupt power to a single home, but a worst-case solar event electromagnetic pulse (EMP) would take an estimated four to ten years to repair and leave most of the United States without power (Federal Energy Regulatory Commission, 2010).

Regardless of the cause, the consequences of a disruption have significant negative implications for our welfare, both in terms of loss of life as well as negative economic impacts (Anderson and Bell, 2012; Rose et al., 1997). Generation facilities are frequently taken online and offline to balance power supply and load demand, but unexpected failure of a generation facility can cause problems (Knaus, 2017). Disruptions to transmission systems, either from the loss of a high-voltage line or a substation, can impede the ability to move bulk power and cause long-distance power outages (Cava, 2017). A disruption to a distribution system causes downstream customers to potentially go without electricity, but these effects are often local in nature.

There is a tactical need to understand the strengths and weaknesses of our own electric grid as well as those of potential adversaries. Domestically, identifying weaknesses in our grid informs our defense efforts so we can minimize the impact of adversarial action against us, because as reporters, politicians, and utility operators know, disruptions are devastating (Williams and Bennett, 2016). From an offensive perspective, we desire to know the effects of targeting an enemy's infrastructure to achieve our tactical objective, but we desire to restrict the consequence to only what's necessary to achieve victory. Militarily, the second order effects of taking out an entire transmission system in an enemy territory might prove too costly. Research has shown that in large scale power outages, ordinary civilians suffer and death rates increase (Anderson and Bell, 2012). If we seek to confine power disruption to as small an area as possible, attacking the transmission system is off the table. Hart et al. (2014) provide a discussion of the tensions and tradeoffs for targeting infrastructure in a

military context.

Prior research and analysis efforts at the Naval Postgraduate School (NPS) have focused primarily on the behavior and response of transmission systems. There are multiple research papers and theses on the subject of transmission system modeling (e.g., Rose, 2007; Salmerón et al., 2012). Comparatively, little effort has been applied to distribution systems.

The focus of this thesis is understanding how a distribution system will respond to the loss of components (e.g., substations), and in particular the presence and size of outages. In response to component failure, a distribution system will adjust its connectivity by opening and closing switches to continue powering as much of the grid as possible. We capture this behavior in a prescriptive decision Alternating Current Power Flow (ACPF) model which changes flow by changing connectivity via switch position adjustments to minimize the amount of load shed.

We implement the ACPF model in the Python programming language (Python Software Foundation, 2017), primarily relying on the Pyomo optimization package (Hart et al., 2012, 2011). We verify model operation by application to a toy model and then expand to a real data set from a large Northeastern utility provider.

1.2 Thesis Structure

Chapter 2 provides cursory overviews of the academic disciplines underpinning this work. Additionally, we review the relevant literature and research pertaining to our analysis. In Chapter 3 we introduce the ACPF model and demonstrate its application with a small series of toy data sets. Chapter 4 describes our application of the model to a standardized test circuit. We conclude in Chapter 5 by summarizing our findings along with recommendations for future research.

THIS PAGE INTENTIONALLY LEFT BLANK

CHAPTER 2:
Background

This chapter provides background information on the disciplines involved in this thesis as well as pertinent previous research.

2.1 Technical Background Overview

Our work encapsulates two major academic domains: mathematical optimization and Electrical Engineering (EE). While it is beyond the scope of this thesis to fully inform the reader on both these subjects, we seek to provide a brief overview to aid reading our work.

2.1.1 Mathematical Programming

Mathematical programming involves theory and methods for solving for extreme points, either maxima or a minima, of functions on sets defined by linear and/or non-linear constraints. The primary objective function for which a maxima or a minima is being found, commonly involves a maximum profit or lowest cost. The constraints are linear equality and inequalities representing limitations imposed on the system, such as how much money can be spent or the capacity limits of a path. For a thorough introduction to optimization and mathematical programming, see the textbook *Optimization in Operations Research* (Rardin, 2016).

2.1.2 Electrical Engineering

For a deeper understanding of EE as it applies to electric power systems we recommend the work *Elements of Power Systems* (Sadhu and Das, 2015).

Electrical transmission and distribution systems are frequently 3-phase Alternating Current (AC) systems. The three phases are conventionally a, b, or c and a given load or line in the network can be any combination of the three phases. The supply and demand quantities in the network are measured in watts, with transmission systems generally operating in Megawatts (Mw) while distribution systems frequently are measured in Kilowatts (Kw).

Generated electricity consists of real and reactive components. Real power produces kinetic work (e.g., motors spinning), while reactive power is the electromagnetic hindrance of electrical processes. Correspondingly, loads in the network consume real and/or reactive power. Individual power lines possess both resistance and reactance, qualities that hinder real and reactive power flow, respectively.

2.2 Previous Research

2.2.1 Attacker-Defender and Defender-Attacker-Defender Analysis

Attacker-Defender (AD) analysis is a two-part optimization problem. The attacker seeks to maximize the minimum value the defender can obtain from the system post attack. There are three key assumptions in AD modeling, "(1) the attacker's and defender's actions are sequential, (2) the attacker has a perfect model of how the defender will (or should) optimally operate the system, even after an attack, and (3) the attacker will manipulate that system to his best advantage" (Brown et al., 2006).

Defender is a bit of a misnomer in an AD model. Nothing is being hardened or made invulnerable to attack; in reality the defender is simply a system user who best operates post-attack. However, it is possible to expand a two-level AD model into a three-level Defender-Attacker-Defender (DAD) model, where the system is initially hardened to preclude or mitigate the most damaging attack (Brown et al., 2006). Afterward and with knowledge of the defensive action, the attacker performs a most damaging attack, and lastly the system operator works to obtain best system performance.

Salmerón et al. (2004) applies attacker-defender optimization supported by a heuristic to an electric power model. They account for a great deal of electrical physics considerations, abstaining from the simplifications of a pure flow model. Their results demonstrate the ability to identify the key components in a network that, if attacked, would be most crippling to operation and simultaneously represent the greatest need for hardening and resiliency efforts. Analysis is performed on Institute of Electrical and Electronics Engineers (IEEE) Reliability Test System (RTS) 96.

Salmerón et al. (2005) introduce a Graphical User Interface (GUI) for electric power infrastructure analysis, named Vulnerability of Electric Grids Analyzer (VEGA), which

is supported by an optimal power flow linear program and an interdiction model based on heuristic algorithms. The heuristic algorithm is used to "find the combination of facilities (generating units, buses, transmission lines, transformers and/or substations) whose destruction would cause the largest or nearly largest disruption in the system at a given point in time, which in turn suggests the system components most in need of hardening" (Salmerón et al., 2005). Tests and analysis are performed on two real world transmission systems. Additionally, a time-series component is incorporated with acknowledgement of peak loading time-frames being the most devastating windows of attack.

Salmerón and Wood (2009) extend prior work to formulate and solve DAD problems for electrical transmission grids, identifying critical components sensitive to terrorist attack. Applying a generalized version of Benders decomposition, Salmerón et al. (2009) identify a set of components whose interdiction causes maximum economic loss to customers. Their test problems "describe a regional power grid in the United States with approximately 5000 buses, 6000 lines, and 500 generators" (Salmerón et al., 2009).

Salmerón et al. (2011) perform DAD analysis on Vandenberg Air Force base and its surrounding area. Their efforts identify the vulnerable components whose destruction would be maximally disruptive to system operation and presume adversaries are aware of those defensive preparations, in turn making maximally destructive attacks. Lastly, the system is optimally operated post-attack. This focus on a Department of Defense (DOD) entity is unique because the surrounding area benefits from excess generation capacity.

Further modeling efforts focus on the Guam Power Authority (GPA), identifying critical sets of components whose destruction would most impede GPA's ability to provide power (Salmerón et al., 2012). Subsequently, these sets of components benefit the most from hardening efforts.

2.2.2 Previous NPS Theses

Analysis on electric power systems using AD and DAD models has been driven and supported by many student theses.

Stathakos (2003) performs research contributing to the development of VEGA. Alvarez (2004) demonstrates empirical speed ups to Benders decomposition on electric grid inter-

diction problems, tested against IEEE RTS networks. Optimality gap reductions occurred alongside speed improvements.

Carnal (2005) further improves on VEGA by inclusion of the Xpres-MP software package, reducing run-time by 65% - 85%.

Schneider (2005) performs DAD analysis on the eastern interconnection transmission grid and determine hardening levels necessary to reduce risk below acceptable levels. Jonart (2008) does follow-on work, making algorithmic improvements, yielding results within 1% of optimality.

Ang (2006) performs a Mixed-integer program (MIP) optimization of electric grid recovery efforts after natural disaster or terrorist attack. Constraints include availability of repair resources, penalties for unserved electricity demand, and repair time planning horizons. Testing is performed on an IEEE 300 bus transmission network.

Rose (2007) develops a mathematical model to identify critical components to defend in an electric grid, given limited resources. Using a pure-flow model for the electric grid, Rose reduces solution times from previous efforts while simultaneously finding solutions that are 40% better.

2.2.3 Damage Anticipation Modeling on Electrical Systems

Guikema et al. (2010) use regression and data mining techniques to estimate required repair time and replacement utility poles and transformers in the wake of electric power infrastructure damage resulting from natural disaster, notably hurricanes. Their efforts are predictive in nature and seek to best prepare responders for repairs after a disruption. Ouyang and Dueñas-Osorio (2014) build a probabilistic model to determine economic, social, technical, and organizational resilience to hurricane damage.

Maliszewski and Perrings (2012) use regression modeling to build spatial outage visualizations and identify geographic factors with strong correlation to minimal outage risks in Phoenix's electrical distribution system. They find a strong correlation of neighborhoods near high priority customers such as hospitals experiencing shortened outages because of "the quality of infrastructure provided and the priority given to restoring supply to those users" (Maliszewski and Perrings, 2012). Proximity to vegetation was statistically signifi-

cant as well while other services, such as police and fire stations or schools, all which were insignificant or negatively correlated.

A variety of natural disasters, notably the 2010 earthquakes in Haiti and Chile, the 2011 earthquake and tsunami in Japan, as well as multiple hurricanes, have served as the sources of data for various resiliency modeling efforts. MacKenzie and Barker (2012) build a regression model and mixed effects model to anticipate rates of recovery post-disruption and anticipate a system's resiliency. Using data from Hurricane Ike, Wei et al. (2013) develop a "spatial-temporal non-stationary random process to model large-scale disruptions of power distribution induced by severe weather." Their stochastic approach yields resiliency estimates for components and identifies dynamic neighborhoods within the network. Kwasinski (2016) performs data analysis and regression modeling to inform future damage anticipation efforts and design considerations for distribution systems.

2.2.4 Optimal Switching and RTS usage

Delgadillo et al. (2010) construct an optimization approach to defend a grid against terrorist attack by calculating the best operator response (e.g., switching) to disruption. Their work is a two-part optimization, first identifying the most damaging terrorist attack, measured in Mw not delivered, and then identify the optimal switch realignment in response to that attack.

Additionally, de Assis et al. (2015) consider optimization of switch allocation for distribution systems. They use a distribution system and identify the ideal locations for switches under various system design constraints. Specifically, their research minimizes the cost of switch allocation, a system design consideration. They also minimize energy not supplied while meeting various regulatory agency reliability requirements and system capacity necessities. Their solutions are determined by "memetic algorithms, supported by well-established genetic algorithm concepts and local search optimization procedures."

The IEEE 118-bus and the RTS 96 test system are studied for optimal transmission system switching with a mixed integer program (Hedman et al., 2009). Their model demonstrates the test networks can be operated to meet N-1 secure standards while simultaneously cutting costs. Another instance of RTS usage is the work of Alguacil et al. (2003) in their transmission expansion planning optimization problem.

THIS PAGE INTENTIONALLY LEFT BLANK

CHAPTER 3:
Model

We develop an alternating current (AC) model for electrical distribution system that integrates switching and adherence to full 3-phase AC mathematics. Instead of suggesting likelihoods of what could happen in a disaster or terrorist scenario, we model what will happen for any disruption or series of disruptions.

3.1 Model Formulation

Our Alternating Current Power Flow (ACPF) model is built in collaboration with our partners at Los Alamos National Laboratory (LANL), notably Harsha Nagarajan and Arthur Barnes, with significant sourcing from their previous work (e.g., Barnes et al., 2017; Nagarajan et al., 2016).

The entirety of our ACPF model is presented in NPS format for a given Power Grid (PG). Discussion of the objective function and constraints follows in section 3.1.2.

3.1.1 Mathematical Formulation

Sets and Indices

$i \in \mathcal{N}$ set of nodes (buses) in PG (alias j)

$\mathcal{E} \subseteq \mathcal{N} \times \mathcal{N}$ set of undirected edges (lines and transformers) in PG

$\mathcal{NT} \subseteq \mathcal{E}$ set of edges without transformers in PG

$\mathcal{S} \subseteq \mathcal{NT}$ set of edges with switches in PG

$\mathcal{A} \subseteq \mathcal{N} \times \mathcal{N}$ set of directed arcs (lines and transformers) in PG

$$(i, j) \in \mathcal{E} \iff (i, j) \in \mathcal{E} \wedge (j, i) \in \mathcal{E}$$

$\mathcal{P} = \{a, b, c\}$ set of phases in PG

$k \in \mathcal{P}_i \subseteq \mathcal{P}$ set of phases on bus i which contains a load or a generator

$\mathcal{P}_{ij} \subseteq \mathcal{P}$ set of phases on line (i,j) in PG

C set of cycles in PG

$\mathcal{N}(C)$ set of nodes in cycle C

$\mathcal{E}(C)$ set of edges in cycle C

Parameters [units]

$\lambda p_{i,k}$ cost for shedding real power at bus i on phase k [$/watt]

$\lambda q_{i,k}$ cost for shedding reactive power at bus i on phase k [$/watt]

$T_{ij,k}$ thermal limit on edge (i,j) for phase k [Amps]

$v^l_{i,k}, v^u_{i,k}$ voltage lower and upper bounds at bus i for phase k [Kv]

$\mathbf{i}$ imaginary number constant

$dp_{i,k} + \mathbf{i}\, dq_{i,k}$ AC power demand at bus i on phase k [Kw and Kvar]

$gp^u_{i,k} + \mathbf{i}\, gq^u_{i,k}$ existing AC power generation capacity at bus i on phase k [Kw and Kvar]

$R_{ij,k} + \mathbf{i}\, X_{ij,k}$ impedance of edge (i,j) on phase k in PG [Ω]

Z_{ij} impedance of edge (i,j), defined as:

$\overline{Z}_{ij} = Z_{ij}e^{\mathbf{i}2\pi/3}$; $\underline{Z}_{ij} = Z_{ij}e^{-\mathbf{i}2\pi/3}$, where, $\overline{Z}_{ij} = \overline{R}_{ij} + \mathbf{i}\overline{X}_{ij}$, $\underline{Z}_{ij} = \underline{R}_{ij} + \mathbf{i}\underline{X}_{ij}$ [Ω]

M_{ij} $M_{ij} = (1.05V^{nom}_j)^2 - (0.95V^{nom}_i)^2\ \forall ij \in \mathcal{E}\ [Volts^2]$

β_{ij} allowed variation in flow between phases on edge (i,j) [0.15 for transformer edges, 1.0 for all other edges]

V^{nom}_i nominal voltage the system is operating at [Kv]

Decision Variables [units, when appropriate]

$v_{i,k}$ voltage at bus i on phase k [Kv]

x_{ij} determines if directed arc (i,j) carries power flow in PG [binary]

$p_{ij,k}$ real AC power flow on arc (i, j) [Kw]

$q_{ij,k}$ reactive AC power flow on arc (i, j) [Kvar]

$lp_{i,k} + \mathbf{i}\, lq_{i,k}$ AC power load that is shed at bus i on phase k

$gp_{i,k} + \mathbf{i}\, gq_{i,k}$ existing AC power generation capacity at bus i on phase k

Formulation

$$\min \sum_{i \in N, k \in \mathcal{P}_i} (\lambda p_{i,k} lp_{i,k} + \lambda q_{i,k} lq_{i,k}) \tag{1}$$

s.t.

Power flow constraints

$$gp_{i,k} - dp_{i,k} + lp_{i,k} = \sum_{ij \in \mathcal{E}} p_{ij,k} - \sum_{ji \in \mathcal{E}} p_{ji,k} \qquad \forall i \in \mathcal{A}, k \in \mathcal{P}_i \tag{2a}$$

$$gq_{i,k} - dq_{i,k} + lq_{i,k} = \sum_{ij \in \mathcal{E}} q_{ij,k} - \sum_{ji \in \mathcal{E}} q_{ji,k} \qquad \forall i \in \mathcal{A}, k \in \mathcal{P}_i \tag{2b}$$

$$(1 - \beta_{ij}) \left(\frac{\sum_{k \in \mathcal{P}_{ij}} p_{ij,k}}{|\mathcal{P}_{ij}|} \right) \leq p_{ij,k} \leq (1 + \beta_{ij}) \left(\frac{\sum_{k \in \mathcal{P}_{ij}} p_{ij,k}}{|\mathcal{P}_{ij}|} \right) \qquad \forall ij \in \mathcal{A}, k \in \mathcal{P}_{ij} \tag{3a}$$

$$(1 - \beta_{ij}) \left(\frac{\sum_{k \in \mathcal{P}_{ij}} q_{ij,k}}{|\mathcal{P}_{ij}|} \right) \leq q_{ij,k} \leq (1 + \beta_{ij}) \left(\frac{\sum_{k \in \mathcal{P}_{ij}} q_{ij,k}}{|\mathcal{P}_{ij}|} \right) \qquad \forall ij \in \mathcal{A}, k \in \mathcal{P}_{ij} \tag{3b}$$

$$p_{ij,k}^2 + q_{ij,k}^2 \leq x_{ij} T_{ij,k}^2 (V_i^{nom})^2 \sqrt{3} \qquad \forall ij \in \mathcal{A}, k \in \mathcal{P}_{ij} \tag{4}$$

$$p_{ij,k} + q_{ij,k} \leq x_{ij} T_{ij,k} V_i^{nom} \sqrt{6} \qquad \forall ij \in \mathcal{A}, k \in \mathcal{P}_{ij} \tag{4a}$$

$$(v_{j,a})^2 - (v_{i,a})^2 + 2(R_{ij}^{aa} p_{ij,a} + X_{ij}^{aa} q_{ij,a} + \overline{R}_{ij}^{ab} p_{ij,b} + \overline{X}_{ij}^{ab} q_{ij,b} + \underline{R}_{ij}^{ac} p_{ij,c} + \underline{X}_{ij}^{ac} q_{ij,c})$$
$$\geq -M_{ij}(1 - x_{ij}) \qquad \forall ij \in \mathcal{NT} \tag{5a}$$

$$(v_{j,b})^2 - (v_{i,b})^2 + 2(R_{ij}^{bb} p_{ij,b} + X_{ij}^{bb} q_{ij,b} + \overline{R}_{ij}^{bc} p_{ij,c} + \overline{X}_{ij}^{bc} q_{ij,c} + \underline{R}_{ij}^{ba} p_{ij,a} + \underline{X}_{ij}^{ba} q_{ij,a})$$
$$\geq -M_{ij}(1 - x_{ij}) \qquad \forall ij \in \mathcal{NT} \tag{5b}$$

$$(v_{j,c})^2 - (v_{i,c})^2 + 2(R^{cc}_{ij} p_{ij,c} + X^{cc}_{ij} q_{ij,c} + \overline{R}^{ca}_{ij} p_{ij,a} + \overline{X}^{ca}_{ij} q_{ij,a} + \underline{R}^{cb}_{ij} p_{ij,b} + \underline{X}^{cb}_{ij} q_{ij,b})$$
$$\geq -M_{ij}(1 - x_{ij}) \qquad \forall ij \in \mathcal{NT} \qquad (5c)$$

$$(v_{j,a})^2 - (v_{i,a})^2 + 2(R^{aa}_{ij} p_{ij,a} + X^{aa}_{ij} q_{ij,a} + \overline{R}^{ab}_{ij} p_{ij,b} + \overline{X}^{ab}_{ij} q_{ij,b} + \underline{R}^{ac}_{ij} p_{ij,c} + \underline{X}^{ac}_{ij} q_{ij,c})$$
$$\leq M_{ij}(1 - x_{ij}) \qquad \forall ij \in \mathcal{NT} \qquad (5d)$$

$$(v_{j,b})^2 - (v_{i,b})^2 + 2(R^{bb}_{ij} p_{ij,b} + X^{bb}_{ij} q_{ij,b} + \overline{R}^{bc}_{ij} p_{ij,c} + \overline{X}^{bc}_{ij} q_{ij,c} + \underline{R}^{ba}_{ij} p_{ij,a} + \underline{X}^{ba}_{ij} q_{ij,a})$$
$$\leq M_{ij}(1 - x_{ij}) \qquad \forall ij \in \mathcal{NT} \qquad (5e)$$

$$(v_{j,c})^2 - (v_{i,c})^2 + 2(R^{cc}_{ij} p_{ij,c} + X^{cc}_{ij} q_{ij,c} + \overline{R}^{ca}_{ij} p_{ij,a} + \overline{X}^{ca}_{ij} q_{ij,a} + \underline{R}^{cb}_{ij} p_{ij,b} + \underline{X}^{cb}_{ij} q_{ij,b})$$
$$\leq M_{ij}(1 - x_{ij}) \qquad \forall ij \in \mathcal{NT} \qquad (5f)$$

$$(0.95V^{nom}_i)^2 \leq v^2_{i,k} \leq (1.05V^{nom}_i)^2 \qquad \forall i \in \mathcal{N}, k \in \mathcal{P}_i \qquad (6)$$

$$0 \leq gp_{i,k} \leq gp^u_{i,k} \qquad \forall i \in \mathcal{N}, k \in \mathcal{P}_i \qquad (7a)$$

$$gq_{i,k} \leq gq^u_{i,k} \qquad \forall i \in \mathcal{N}, k \in \mathcal{P}_i \qquad (7b)$$

$$-gq_{i,k} \leq gq^u_{i,k} \qquad \forall i \in \mathcal{N}, k \in \mathcal{P}_i \qquad (7c)$$

$$lp_{i,k} \leq dp_{i,k} \qquad \forall i \in \mathcal{N}, k \in \mathcal{P}_i \qquad (8a)$$

$$lq_{i,k} \leq dq_{i,k} \qquad \forall i \in \mathcal{N}, k \in \mathcal{P}_i \qquad (8b)$$

Topology constraints

$$\sum_{ij \in \mathcal{E}(C)} x_{ij} \leq |\mathcal{N}(C)| - 1 \qquad \forall C \qquad (9)$$

$$x_{ij} + x_{ji} \leq 1 \qquad \forall (i,j) \in \mathcal{E} \qquad (10a)$$

$$x_{ij} + x_{ji} \geq 1 \qquad \forall (i,j) \in \mathcal{E} \setminus \mathcal{S} \qquad (10b)$$

3.1.2 Model Discussion

The objective function (1) minimizes the cost associated with all real and reactive load shed due to the loss of generation capacity at bus i. The cost parameters, $\lambda p_{i,k}$ and $\lambda q_{i,k}$ (nominally set to 1) scale the total value of Kw and Kilovolt-ampere reactive (Kvar) shed by the model.

Constraints (2a) and (2b) maintain balance of flow throughout the network, node by node, between generation, load, and load shedding, for real and reactive power, respectively.

Constraints (3a) and (3b) ensure that real and reactive power flows for each phase are within stated tolerances. A large difference in flow on a single line between two phases isn't desirable from an EE perspective. The β_{ij} terms are tolerance parameters: the higher the β_{ij} value, the wider the tolerance between phases that is allowed.

Constraint (4) ensures the thermal limits of line (i, j) are not exceeded. These limits are enforced only if a line is being used (i.e., $x_{ij} = 1$). Constraint (4a) is a linear version to allow each x_{ij} to control whether flow is permitted on arc (i, j).

Constraints (5a) through (5f) account for flow losses across all possible phase combinations on line (ij) due to resistance and reactance values for that line. Again, these constraints are enforced only if a line is being used (i.e., $x_{ij} = 1$).

Constraint (6) maintains voltage at node i within 95% to 105% of the nominal voltage for that node, as mapped by its location from the nearest upstream transformer.

Constraints (7a), (7b), and (7c) ensure nodes only generate real and/or reactive power if capable, as appropriate.

Constraints (8a) and (8b) only allow load to be shed at nodes with real or reactive load. This prevents the formulation from spuriously shedding load at nodes without load, simply to satisfy constraint mathematics.

Constraint (9) precludes cycles in the network by ensuring the number of active edges in a cycle is one less than the number of edges in that cycle. This constraint is implemented differently than the others. Initially, we solve the ACPF model without the cycle breaking constraint active. Once a solution is obtained we analyze it to identify cycles within that solution. For each cycle in the incumbent solution, a copy of constraint (9) is added and then the ACPF model is solved again.

Constraint (10a) ensures there is flow in at most one direction (namely, on one arc) for a given edge, and constraint (10b) ensures that edges without a switch are active in at least one direction. If the switch on edge (i, j) is open, then both x_{ij} and x_{ji} will be zero.

3.2 Model Implementation

The model is built in the Python programming language, an interpreted, high-level, general purpose programming language (Python Software Foundation, 2017). The modular and flexible nature of Python enabled us to integrate all computational tasks within a single program. The data read and processing steps use several standard Python packages, including `json`, `numpy`, and `math` packages, as well as `networkx` (Hagberg et al., 2008) for analysis. The mathematical program is implemented in Pyomo, a "Python-based, open-source optimization modeling language with a diverse set of optimization capabilities" (Hart et al., 2012, 2011).

Our test networks and the real life network are all in JavaScript Object Notation (JSON) format (Ecma International, 2017), with three dictionaries in the data file, one for the nodes, one for the edges in the network, and another for more detailed information on the nodes. JSON, consisting of name and value pairs for its data storage is a natural fit for the Python (and Pyomo) objects we use to construct the model.

After constructing all of the Python storage objects necessary for the model we have two primary loops to prepare the data, one for the nodes and one for the edges. During these loops we read in all of the requisite details for the distribution system. First, we read in node details including attributes such as the type of node, e.g., substation, shunt capacitor, or load, a unique node identification number, and specific data items such as $dp_{i,k}$, $dq_{i,k}$, $gp^{u}_{i,k}$, $v^{l}_{i,k}$, and more. Next, we read in data for the lines (i.e., edges) in the system. We capture the $R_{ij,k}$ and $X_{ij,k}$ for lines, which nodes in the network a given line connects, and the number of phases in a line. For lines that are transformers we capture the voltage difference across the transformer and map these voltages through the network as V_i^{nom}.

We store all data in Python dictionaries. Dictionaries are an ideal storage medium for the network data because their structure uses key-value pairs and in this case we use the unique node identification number to index node data, and the (tail, head) node identification pairs for an edge to index edge data. Furthermore, Python dictionaries naturally integrate with the Pyomo optimization package for forming Pyomo objects. For example, once a dictionary is created with $R_{ij,k}$, it can be fed directly to the Pyomo resistance object.

Once the data is read in and prepared, we build the ACPF model in Pyomo and solve it with

the CPLEX solver (IBM, 2017).

3.3 Model Testing

We begin with a basic test circuit that has no cycles or switches, a minor design simplification to facilitate incremental model construction. A depiction of the basic test circuit appears in Figure 3.1, with associated parameters in Table 3.1 and Table 3.2.

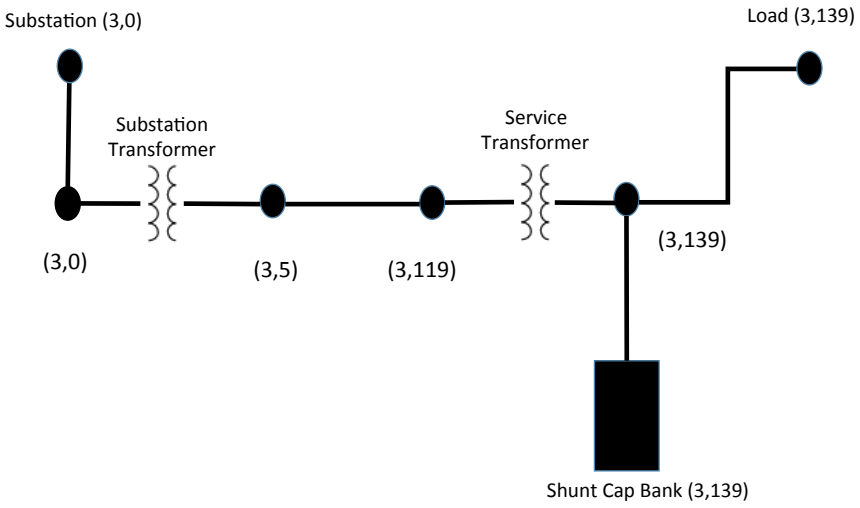

The Basic Test Circuit consists of a substation with functionally infinite capacity, a transformer, connective line leading to a service transformer, and a commercial grade customer with moderate loading and a shunt capacitor bank. When operated, no load should be shed in this test network.

Figure 3.1. Basic Test Circuit

3.4 Model Performance on Basic Test Circuit

The ACPF model, running on an early 2015 MacBook Pro with a 2.7 GHz i5 processor, solves the basic test circuit in less than a second. The objective function (1) returns a result of 0.00 corresponding to zero load shed, as anticipated. We observe $p_{ij,k}$ flows from the

Table 3.1. Basic Test Circuit Node Data

Node	Type	$gp^u_{i,k}$	$gq^u_{i,k}$	$dp_{i,k}$	$dq_{i,k}$	V_i^{nom}
(3,0)	Substation	∞	∞	0	0	69
(3,5)	Connection	0	0	0	0	7.62
(3,119)	Connection	0	0	0	0	7.62
(3,139)	Load, Shunt capacitor	0	400	57.55 (a) 55.48 (b) 60.65 (c)	29.29 (a) 27.51 (b) 30.78 (c)	0.277

Load for each phase (a-c) indicated explicitly

Table 3.2. Basic Test Circuit Edge Data

Edge	Type	Phases	$T_{ij,k}$	$R_{ij,k}$	$X_{ij,k}$
(3,0),(3,5)	Transformer	a, b, c	120.773	0.0217	0.3548
(3,5),(3,119)	Line	a, b, c	498.75	0.1334 (a) 0.1354 (b) 0.1343 (c)	0.3124 (a) 0.3053 (b) 0.3089 (c)
(3,119),(3,139)	Line	a, b, c	32.808	0.0009	0.0053

$R_{ij,k}$ and $X_{ij.k}$ for each phase listed explicitly when variations exist.

substation to the load of 57.55, 55.48, and 60.65 Kw for phases a, b, and c, respectively, values matching the demands in node (3,139).

Due to the presence of a shunt capacitor bank on node (3,139) all reactive demand is satisfied locally at the commercial customer, resulting in no $q_{ij,k}$ flow. Iterative testing, namely removal of the shunt capacitor bank, causes $q_{ij,k}$ flow (in Kvar) satisfying all $dq_{i,k}$. This behavior confirms proper ACPF model operation regarding reactive power flow as well.

At this point our ACPF model has performed as expected on the basic test circuit, successfully operating while adhering to power flow constraints (2a) through (8b).

3.5 Model Testing With Cycles

Once satisfied with operation on the basic test circuit we added switching controls and the cycle breaking constraint (9) to complete implementation of the formulation in our ACPF

model. At this point we build a basic test circuit with a cycle and switches for testing, as depicted in Figure 3.2, with associated data in Table 3.3 and Table 3.4.

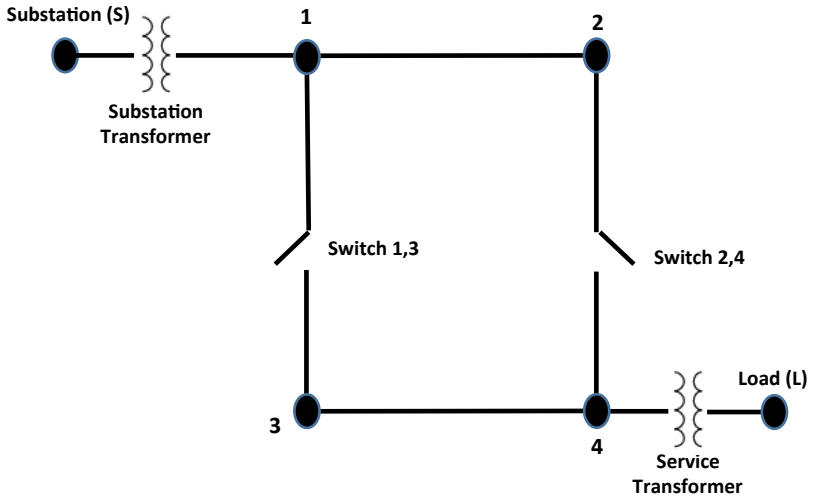

The Basic Test Circuit With Cycle consists of a substation with functionally infinite capacity and a moderate load, each with their own transformer. Between them is a cycle of four nodes, with two of the four edges containing switches. Unlike the Basic Test Circuit, there is no shunt capacitor at the load.

Figure 3.2. Basic Test Circuit with Cycle

Table 3.3. Basic Test Circuit with Cycle Node Data

Node	Type	$gp^u_{i,k}$	$gq^u_{i,k}$	$dp_{i,k}$	$dq_{i,k}$	V_i^{nom}
Sub	Substation	∞	∞	0	0	100
1	Connection	0	0	0	0	10
2	Connection	0	0	0	0	10
3	Connection	0	0	0	0	10
4	Connection	0	0	0	0	10
Load	Load	0	0	30.0	20.0	1

Loading for each phase a - c is identical.

Table 3.4. Basic Test Circuit with Cycle Edge Data

Edge	Type	Phases	$T_{ij,k}$	$R_{ij,k}$	$X_{ij,k}$
Sub,1	Transformer	a, b, c	100	0.0217	0.3548
1,2	Line	a, b, c	100	0.1334	0.3124
1,3	Line	a, b, c	100	0.1334	0.3124
2,4	Line	a, b, c	100	0.1334	0.3053
3,4	Line	a, b, c	100	0.1343	0.3089
4,Load	Transformer	a, b, c	100	0.0009	0.0053

$R_{ij,k}$ and $X_{ij,k}$ for each phase listed explicitly when variations exist.

The Basic Test Circuit with Cycle contains realistic R_{ij} and X_{ij} values, drawn from real networks. Possessing a single load with its own service transformer and a substation with functionally infinite $gp_{i,k}$ and $gq_{i,k}$, the basic test circuit with cycle is electrically sound and designed to shed no load when solved.

3.6 Model Performance on Basic Test Circuit with Cycle

Our model solves the basic test circuit with cycle initially, not enforcing the cycle breaking constraint, resulting in the behavior summarized in Table 3.5.

Table 3.5. Basic Test Circuit with Cycle Results before Cycle Breaking Constraint

Edge	Type	Switch / Position	x_{ij}	$p_{ij,k}$	$q_{ij,k}$
Sub,1	Transformer	False, N/A	1	30.0	20.0
1,2	Line	False, N/A	1	15.0	10.0
1,3	Line	True, Closed	1	15.0	10.0
2,4	Line	True, Closed	1	15.0	10.0
3,4	Line	False, N/A	1	15.0	10.0
4,Load	Transformer	False, N/A	1	30.0	20.0

$p_{ij,k}$ and $q_{ij,k}$ flows the same for all phases.

At this point, we check the incumbent solution for cycles (using the `networkx` package) and identify the cycle consisting of nodes 1, 2, 3, and 4. The cycle breaking constraint (9) is enforced and the ACPF model runs again, this time producing a solution with no cycles and zero load shed, as summarized in Table 3.6. Cycle breaking is restricted to opening a switch on lines that have switches.

Table 3.6. Basic Test Circuit with Cycle Results after Cycle Breaking Constraint

Edge	Type	Switch / Position	x_{ij}	$p_{ij,k}$	$q_{ij,k}$
Sub,1	Transformer	False, N/A	1	30.0	20.0
1,2	Line	False, N/A	1	0.0	0.0
1,3	Line	True, Closed	1	30.0	20.0
2,4	Line	True, Open	0	0.0	0.0
3,4	Line	False, N/A	1	30.0	20.0
4,Load	Transformer	False, N/A	1	30.0	20.0

$p_{ij,k}$ and $q_{ij,k}$ flows the same for all phases.

As can be observed, the cycle breaking constraint has forced the switch on line 2,4 to open. Flow redirected to meet demand while avoiding a cycle being present in the network.

3.7 Model Validation

Having tested our ACPF model's basic functions we test it against an IEEE RTS network for validation. The IEEE RTS is a standardized test circuit whose behavior is well understood by researchers and academia. Furthermore, phase changes, multiple branching paths, and uneven loading make it a more robust test case than the basic test networks used thus far. Observing proper behavior of the ACPF model on the RTS network serves as validation to our modeling and these efforts are described in Chapter 4.

THIS PAGE INTENTIONALLY LEFT BLANK

CHAPTER 4:
Results

4.1 IEEE RTS 13-bus feeder

We choose the IEEE RTS 13 node test feeder because it is relatively small and frequently used to test analysis software (IEEE Power and Energy Society, 2017). Furthermore, the network itself mimics real world distribution and is "characterized by being short, relatively highly loaded, a single voltage regulator at the substation, overhead and underground lines, shunt capacitors, an in-line transformer, and unbalanced loading" (IEEE Power and Energy Society, 2017). A network with these characteristics will test many facets of our model in a more robust capacity than the test networks in Chapter 3. The network is constructed without the potential for cycles however, so our cycle breaking constraint is not exercised when solving the IEEE RTS 13 node test feeder. The circuit is depicted in Figure 4.1.

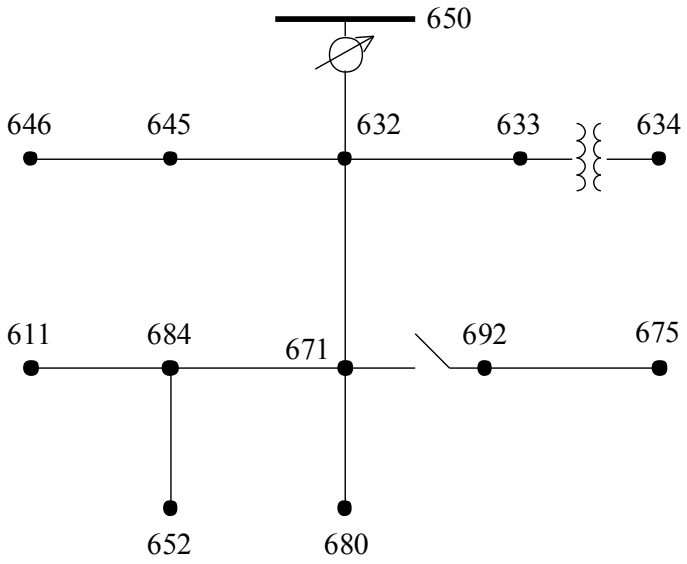

Figure 4.1. IEEE 13 Node Test Feeder. The substation is at node 634 with its transformer between node 634 and 633. A voltage regulator exists between node 632 and 650 but has no impact on network behavior within our model because node 650 is an unloaded bus.

Full electrical characteristics for the 13 node test feeder can be found on the IEEE Power and Energy Society website (IEEE Power and Energy Society, 2017). The basic characteristics and those specifically pertinent to our ACPF model are described in Tables 4.1 and 4.2. Additionally, there is a distributed load in the IEEE 13 node test feeder along the line between nodes 632 and 671. We capture this load as an extra node named "dload," existing equidistant between nodes 632 and 671. The distributed load node has $dp_{i,k}$ values of 10, 38, and 68, with $dq_{i,k}$ values of 17, 66, and 117, all for phases *a*, *b*, and *c,* respectively.

Table 4.1. IEEE 13 Node Test Feeder Node Data

Node	Type	$gp^u_{i,k}$	$gq^u_{i,k}$	$dp_{i,k}$	$dq_{i,k}$	V_i^{nom}
634	Substation, Load	∞	∞	160(a) 120(b,c)	110(a) 90(b,c)	115
633	Connection	0	0	0	0	4.16
632	Connection	0	0	0	0	4.16
650	Connection	0	0	0	0	4.16
645	Load	0	0	170(b)	125(b)	4.16
646	Load	0	0	230(b)	132(b)	4.16
671	Load	0	0	385(a,b,c)	220(a,b,c)	4.16
684	Connection	0	0	0	0	4.16
652	Load	0	0	128(a)	86(a)	4.16
611	Load, Shunt capacitor	0	100(c)	170(c)	80(c)	4.16
680	Connection	0	0	0	0	4.16
692	Load	0	0	170(c)	151(c)	4.16
675	Load, Shunt capacitor	0	200 (a,b,c)	485(a) 68(b),290(c)	190(a) 60(b),212(c)	4.16

Load for each phase (a-c) indicated explicitly

Table 4.2. IEEE 13 Node Test Feeder Edge Data

Edge	Type	Phases	$T_{ij,k}$
634,633	Transformer	a, b, c	1500
633,632	Line	a, b, c	340
632,650	Line	a, b, c	730
632,645	Line	b, c	230
645,646	Line	b, c	230
632,dload	Line	a, b, c	730
dload,671	Line	a, b, c	730
671,684	Line	a, c	230
684,611	Line	c	230
684,652	Line	a	165
671,680	Line	a, b, c	730
671,692	Line	a, b, c	1500
692,675	Line	a, b, c	260

$R_{ij,k}$ and $X_{ij.k}$ for the network are 3 x 3 matrices. We refer our readers to the IEEE RTS reference materials for specific values.

The network structure and parameters are built into the JSON format our associates at LANL are using and which our model is built to read.

4.2 IEEE 13 Node Test Feeder Performance

The IEEE RTS 13 node test feeder runs in a little over a second and returns an optimal solution objective function value of 0.00, a result our associates at LANL confirmed. Electrical behavior is captured in Table 4.3.

Table 4.3. IEEE 13 Node Test Feeder Edge Results

Edge	Type	x_{ij}	$p_{ij,k}$	$q_{ij,k}$
634,633	Transformer	1	1015 (a) 919 (b) 1132 (c)	381.91 (a) 515 (b) 451 (c)
633,632	Line	1	1015 (a) 919 (b) 1132 (c)	381.91 (a) 515 (b) 451 (c)
632,650	Line	1	0.00	0.00
632,645	Line	1	400 (b)	257 (b)
645,646	Line	1	230 (b)	132 (b)
632,dload	Line	1	1015 (a) 519 (b) 1132 (c)	381.91 (a) 258 (b) 451 (c)
dload,671	Line	1	998 (a) 453 (b) 1015 (c)	371.91 (a) 220 (b) 383 (c)
671,684	Line	1	128 (a) 170 (c)	86 (a) 0.00 (c)
684,611	Line	1	170 (c)	0.00 (c)
684,652	Line	1	128 (a)	86 (a)
671,680	Line	1	0.00	0.00
671,692	Line	1	485 (a) 68 (b) 460 (c)	115.11 (a) 21.33 (b) 197 (c)
692,675	Line	1	485 (a) 68 (b) 290 (c)	65.91 (a) 0.00 (b) 12 (c)

Our ACPF model demonstrates full functionality at this point, managing cycles, optimal switching, and returning expected operational results on a standardized test circuit.

Additionally, running the ACPF model against variations in our test networks (e.g., removing components, constraining electrical parameters, and varying loading amounts) produced electrical results we would expect for these variations.

4.3 Expansion of IEEE 13 Node Test Feeder

Our model is ultimately about performing analysis on distribution systems under the stress of disruption. With that in mind, we build an expanded version of the IEEE 13 node test feeder, essentially cloning the network, with "a" and "b" versions of each node and line. The two versions connect via a line from node 671a to 671b. This 3-phase line contains a switch which is open under normal operating conditions. This expanded IEEE 13 node test feeder is depicted in Figure 4.2

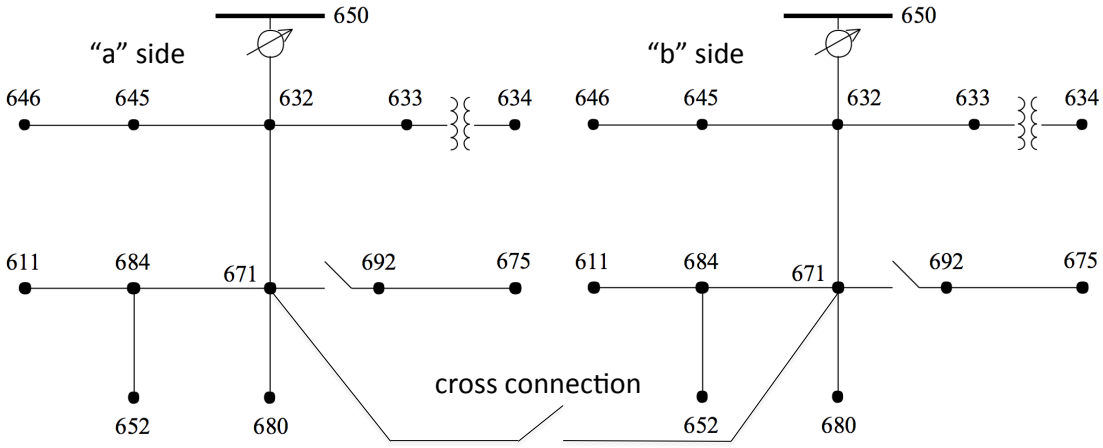

The duplicated 13 node test feeder with "a" and "b" sides, connected by a line between nodes 671a and 671b. Electrical parameters for both sides are the same as the original IEEE 13 node test feeder, described in Tables 4.1 and 4.2. The cross connection line is 3-phase with R_{ij} and X_{ij} values copied from line 692-675. The T_{ij} value is very low at 15 amps.

Figure 4.2. Duplicated 13 Node Test Feeder

When given to our ACPF model the duplicated IEEE 13 node test feeder sheds no load, an expected result since the single version met all load demands. In essence, we have parallel instances of the previous test network and each one saw commensurate electrical behavior, analogous to the results in Table 4.3 for both the "a" and "b" sides. Our next

step is to consider model performance and distribution system behavior in the presence of a disruption.

Our chosen disruption is failure of the "b" side substation, essentially removing it from the network. Running the model with this disruption results in all "a" side load satisfied and the cross connection switch to close. Including the cross-connection, only a handful of lines on the "b" side have flow. Their values are captured in Table 4.4.

Table 4.4. Duplicated IEEE 13 Node Test Feeder Edge Results

Edge	Type	x_{ij}	$p_{ij,k}$	$q_{ij,k}$
671a,671b	Line	1	58.07	58.07
671b,dload_b	Line	1	9.52 (a) 38.82 (b) 41.40 (c)	5.29 (a) 13.90 (b) 18.24 (c)

$p_{ij,k}$ and $q_{ij,k}$ flows the same for all phases unless explicitly listed.

Due to relatively low thermal limit we imposed on the 671a - 671b connection, most of the "b" side goes without power and the model returns an objective function value of 4689.38. We are not surprised by this amount of load shed given the parameters we assigned the cross-connection.

4.4 Model Performance Overview

At this point the model has demonstrates the capability to analyze standardized test circuits in the presence of network disruptions. Electrical parameters behave as expected and operation of any distribution system can be optimized by the ACPF model in an effort to minimize load shed. We provide recommendations for follow-on work and additional model applications in Chapter 5.

CHAPTER 5:
Conclusions and Follow-on Work

5.1 Conclusions

Working within a Python and Pyomo environment with CPLEX as a solver, our model demonstrates the ability to find an optimal network configuration and associated power flow for a 3-phase electrical distribution system. Our ACPF model can handle phase changes, varying and imbalanced loads, real and reactive demand, switch operation, and ensures the network is configured as a spanning tree to meet standard distribution system behavior.

The novelty in our work is due to the focus on distribution systems. The model receives input from a JSON data structure used by the individuals at LANL working on infrastructure analysis. This allows for downstream use. Furthermore, the free and open-source nature of the Python programming language makes our work easily accessible for additional research.

Alternating current is inherently non-linear. That said, the mathematics of the model are linearized, with the exception of constraint (4) which is non-linear. Testing and experimentation revealed that the non-linear structure of constraint (4) allowed for nonsensical solutions when implemented independently. As such, we identified the need to build and include constraint (4a). Doing so achieves correct results from the test networks and the IEEE RTS 13 node test feeder.

5.2 Follow-on Work

Our associates at LANL have a detailed and highly comprehensive dataset from a real northeastern utility provider. Our test networks and IEEE RTS 13 node test feeder are built in the same JSON format as the real-world data, facilitating model application to the real world data after some preliminary data cleaning.

The real-world dataset contains 52 substations, 73,304 loads, and several hundred thousand nodes and arcs. There is interest in systematically triggering failure of substations and capturing network behavior after the ACPF model runs. This analysis would yield data for

subsequent vulnerability analysis as test and training sets. Furthermore, it would inform us regarding distribution system behavior in the presence of substation failure, a topic of interest to various government agencies.

To facilitate future work investigating the behavior of distribution systems in the presence of adverse events, the model should be augmented to more easily disable part of the distribution system being analyzed. At present, the data itself needs to be modified to break a line or disable a substation. An update with the ability to pass in a component identification number as a function argument for disruption purposes would greatly simplify this process.

Lastly, our ACPF model is built as a single Python function, allowing for easy incorporation into AD and DAD analysis. Analysis of this nature would yield insight to the system vulnerabilities of any distribution network and the corresponding hardening efforts of the greatest benefit.

List of References

Alguacil, N., A. Motto, A. Conejo. 2003. Transmission expansion planning: A mixed-integer LP approach. *IEEE Transactions on Power Systems* **18**(3) 1070–1077.

Alvarez, R. E. 2004. Interdicting Electrical Power Grids. Ph.D. thesis, Naval Postgraduate School, Monterey, CA.

Anderson, G. B., M. L. Bell. 2012. Lights out: impact of the August 2003 power outage on mortality in New York, NY. *Epidemiology (Cambridge, Mass.)* **23**(2) 189.

Ang, C. C. 2006. Optimized Recovery of Damaged Electrical Power Grids. Ph.D. thesis, Naval Postgraduate School, Monterey, CA.

Barnes, A., H. Nagarajan, E. Yamangil, R. Bent, S. Backhaus. 2017. Last accessed July 10, 2017. https://arxiv.org/abs/1705.08229.

Brown, G., M. Carlyle, J. Salmerón, K. Wood. 2006. Defending Critical Infrastructure. *Interfaces* **36**(6) 530–544.

Carnal, D. D. 2005. An Enhanced Implementation of Models for Electric Power Grid Interdiction. Ph.D. thesis, Naval Postgraduate School, Monterey, CA.

Cava, M. 2017. Last accessed Aug 6, 2017. https://www.usatoday.com/story/news/nation/2017/04/21/power-outages-slam-san-francisco-90000-affected/100749708/.

de Assis, L. S., J. F. Vizcaı, F. L. Usberti, C. Lyra, C. Cavellucci, F. J. Von Zuben. 2015. Switch allocation problems in power distribution systems. *IEEE Transactions on Power Systems* **30**(1) 246–253.

Delgadillo, A., J. Arroyo, N. Alguacil. 2010. Analysis of Electric Grid Interdiction with Line Switching. Tech. rep., Piscataway, NJ.

Department of Homeland Security. 2017. Last accessed Jul 10, 2017. https://www.dhs.gov/what-critical-infrastructure.

Ecma International. 2017. ECMA-404 The JSON Data Interchange Standard. Last accessed Jul 8, 2017. http://www.json.org/.

Federal Energy Regulatory Commission. 2010. Last accessed Aug 6, 2017. https://www.ferc.gov/industries/electric/indus-act/reliability/cybersecurity/ferc_executive_summary.pdf.

Guikema, S., S. Quiring, S. Han. 2010. Prestorm Estimation of Hurricane Damage to Electric Power Distribution Systems. *Risk analysis* **30**(12) 1744–1752.

Hagberg, A., P. Swart, D. S. Chult. 2008. Exploring network structure, dynamics, and function using NetworkX. G. Varoquaux, T. Vaught, J. Millman, eds., *Proceedings of the 7th Python in Science Conference (SciPy)*. Pasadena, CA, 11–15.

Hart, S.D., J.L. Klosky, S. Katalenich, B. Spittka, E. Wright. 2014. Infrastructure and the Operational Art: A Handbook for Understanding, Visualizing, and Describing Infrastructure Systems. Tech. Rep. ERDC/CERL TR-14-14, US Army Engineer Research and Development Center (ERDC), Champaign, IL.

Hart, W. E., C. Laird, J. Watson, D. L. Woodruff. 2012. *Pyomo–optimization modeling in python*, vol. 67. Springer Science & Business Media.

Hart, W. E., J. Watson, D. L. Woodruff. 2011. Pyomo: modeling and solving mathematical programs in python. *Mathematical Programming Computation* **3**(3) 219–260.

Hedman, K., R. O'Neill, E. Fisher, S. Oren. 2009. Optimal Transmission Switching With Contingency Analysis. *IEEE Transactions on Power Systems* **24**(3) 1577–1586.

IBM. 2017. IBM ILOG CPLEX V12.6.3.0, User's Manual for CPLEX. Last accessed: 10 Aug 2017. http://pic.dhe.ibm.com/infocenter/cosinfoc/v12r6/index.jsp.

IEEE Power and Energy Society. 2017. Last accessed Aug 25, 2017. https://ewh.ieee.org/soc/pes/dsacom/testfeeders/.

Jonart, D. 2008. Interdicting the United States Power Grid: A Revision Incorporating Exact Solutions. Master's thesis, Naval Postgraduate School, Monterey, CA.

Knaus, C. 2017. Last accessed Aug 6, 2017. https://www.theguardian.com/environment/2017/feb/23/gas-fired-power-plants-failed-during-nsw-heatwave-report-reveals.

Kwasinski, A. 2016. Quantitative Model and Metrics of Electrical Grids' Resilience Evaluated at a Power Distribution Level. *Energies* **9**(2) 93.

MacKenzie, C., K. Barker. 2012. Empirical Data and Regression Analysis for Estimation of Infrastructure Resilience, with Application to Electric Power Outages. *Journal of Infrastructure Systems* **19**(1) 25–35.

Maliszewski, P., C. Perrings. 2012. Factors in the Resilience of Electrical Power Distribution Infrastructures. *Applied Geography* **32**(2) 668–679.

Nagarajan, H., E. Yamangil, R. Bent, P. van Hentenryck, S. Backhaus. 2016. Optimal Resilient Transmission Grid Design. *Power Systems Computation Conference (PSCC), 2016*. IEEE, 1–7.

Nuclear Regulatory Commission. 2013. Last accessed Aug 6, 2017. https://www.nrc.gov/reading-rm/doc-collections/fact-sheets/3mile-isle.pdf.

Ouyang, M., L. Dueñas-Osorio. 2014. Multi-dimensional hurricane resilience assessment of electric power systems. *Structural Safety* **48** 15–24.

Python Software Foundation. 2017. Last accessed July 22, 2017. https://www.python.org/.

Rardin, R. L. 2016. *Optimization in Operations Research*. 2nd ed. Pearson, London, UK.

Rose, A., J. Benavides, S. Chang, P. Szczesniak, D. Lim. 1997. The Regional Economic Impact of an Earthquake: Direct and Indirect Effects of Electricity Lifeline Disruptions. *Journal of Regional Science* **37**(3) 437–458.

Rose, R. W. 2007. Defending Electrical Power Grids. Ph.D. thesis, Naval Postgraduate School, Monterey, CA.

Sadhu, K., S. Das. 2015. *Elements of Power Systems*. 1st ed. CRC Press, Boca Raton, FL.

Salmerón, J., D. Alderson, G. Brown. 2011. Resilience Report: Electric Power Infrastructure Supporting Mission Assurance At Vandenberg Air Force Base (U). Tech. rep., Naval Postgraduate School, Monterey, CA.

Salmerón, J., D. Alderson, G. Brown, K. Wood. 2012. Resilience Report: The Guam Power Authority Electric Power Grid: Analyzing Vulnerability to Physical Attack (U). Tech. rep., Naval Postgraduate School, Monterey, CA.

Salmerón, J., K. Wood. 2009. Final Report on DOE Research Project DE-AI02-05ER25670: Reducing the Vulnerability of Electric Power Grids to Terrorist Attacks. Tech. rep., Naval Postgraduate School, Monterey, CA.

Salmerón, J., K. Wood, R. Baldick. 2004. Analysis of Electric Grid Security Under Terrorist Threat. *IEEE Transactions on Power Systems* **19**(2).

Salmerón, J., K. Wood, R. Baldick. 2005. Optimizing Electric Grid Design Under Asymmetric Threat (III). Tech. rep., Naval Postgraduate School, Monterey, CA.

Salmerón, J., K. Wood, R. Baldick. 2009. Worst-case interdiction analysis of large-scale electric power grids. *IEEE Transactions on power systems* **24**(1) 96–104.

Schneider, T. 2005. Analysis of the Interdiction and Protection of the United States Power Grid. Master's thesis, Naval Postgraduate School, Monterey, CA.

Smith, R. 2014. Last accessed Jun 7, 2017. https://www.wsj.com/articles/assault-on-california-power-station-raises-alarm-on-potential-for-terrorism-1391570879.

Stathakos, D. 2003. An enhanced graphical user interface for analyzing the vulnerability of electrical power systems to terrorist attacks. Ph.D. thesis, Monterey, California. Naval Postgraduate School.

Webley, K. 2012. Last accessed Aug 6, 2017. http://nation.time.com/2012/11/26/hurricane-sandy-one-month-later/.

Wei, Y., C. Ji, F. Galvan, S. Couvillon, G. Orellana. 2013. Dynamic modeling and resilience for power distribution. *Smart Grid Communications (SmartGridComm), 2013 IEEE International Conference on*. IEEE, 85–90.

White House. 2013. Presidential Policy Directorate 21: Critical Infrastructure Security and Resilience. Last accessed Jul 10, 2017. https://obamawhitehouse.archives.gov/the-press-office/2013/02/12/presidential-policy-directive-critical-infrastructure-security-and-resil.

Williams, K. B., C. Bennett. 2016. Last accessed Aug 7, 2017. http://thehill.com/policy/cybersecurity/281494-why-a-power-grid-attack-is-a-nightmare-scenario.

Initial Distribution List

1. Defense Technical Information Center
   Ft. Belvoir, Virginia

2. Dudley Knox Library
   Naval Postgraduate School
   Monterey, California